Single-Column Climate Model Simulation of SHEBA in Winter

J. O. Pinto, J. A. Curry, and A. H. Lynch
Program in Atmospheric and Oceanic Sciences
University of Colorado
Boulder, Colorado

Introduction

The wintertime Arctic environment presents several challenges for climate model parameterizations. The extreme cold temperatures shift the peak of the Planck Function to longer wavelengths where the atmosphere has less well-known absorption characteristics. Extremely low water vapor amounts result in what is known as a "dirty window" at wavelengths greater than 12 microns, which is made more important by the shift in the Planck Function related to the cold temperatures. The extreme cold also allows for the formation of ice clouds throughout the atmospheric column. The occurrence of mixed-phase clouds in the boundary layer is also common. It is hypothesized that these clouds can be maintained for extended periods of time due to strong radiative cooling and a lack of ice-forming nuclei (Pinto 1998). Extreme static stability in the form of strong surface-based temperature inversions are the rule in winter, which makes it difficult to simulate the turbulent transport of heat and moisture between the surface and the atmosphere.

In this study, a single-column model (SCM) is employed to evaluate its treatment of radiative transfer and cloud microphysics under nominal Arctic wintertime conditions observed during November at the Surface HEat Budget of the Arctic Ocean (SHEBA) site. The effect of varying the temperature-dependence of cloud phase and the treatment of the radiative properties of clouds on the surface energy budget is determined. In addition, an improved radiative transfer scheme developed for climate modeling, the Rapid Radiative Transfer Model or RRTM (Mlawer et al. 1997), is evaluated under the typical cold and dry conditions occurring over the Arctic ice pack in winter.

Observations

The SHEBA site consists of a Canadian icebreaker, the Des Groseilliers, which supports several instruments onboard and surrounding the ship. The icebreaker was moored to a thicker-than-average multiyear ice floe in the Beaufort Sea.

By November, the station had drifted westward to approximately 76° N, 146° W. The icebreaker housed both a 35-GHz cloud radar and a dual-polarization backscatter unattended lidar (DABUL). The cloud radar is used to determine cloud boundaries and cloud fraction while the lidar may be used to discriminate particle phase. Several meteorological observing stations were set up on the surrounding ice floes. These include the 10-m tower, which measures mean and turbulent quantities at several heights in the surface layer and several flux-Portable Automated Mesonet (PAM) stations, which measure mean and turbulent quantities at 2 m only. Both stations measure the net shortwave and longwave radiative fluxes as well.

Figure 1 shows the evolution of the observed surface temperature, T_{sfc}, and 10-m air temperature over a 2-day period during which sky conditions changed from clear to cloudy. The cloud radar indicates that cloud began moving in around 0700 Universal Time Coordinates (UTC) (Figure 2). This corresponds with a jump in the T_{sfc} of nearly 10° K in a 2 hour period! The strong static stability near the surface is removed over the same period of time. It is noted that the T_{sfc} actually exceeds the 10-m air temperature for an extended period of time while clouds are present. The T_{sfc} comes into near-equilibrium with the low cloud layer at 258° K to 260° K, then gradually decreases as the low cloud dissipates to a new equilibrium of 253° K beneath the higher cloud layer.

Baseline Model Description

A column version of the Arctic Region Climate System Model (ARCSyM) has been developed for testing GCM parameterizations in the Arctic (Pinto et al. 1998). The full three-dimensional version of ARCSyM is described in detail by Lynch et al. (1995).

The cloud microphysics are modeled using the bulk parameterization developed by Hsie (1984), which uses just two prognostic equations: one for cloud water and one for precipitation. A threshold temperature (273.16° K) is
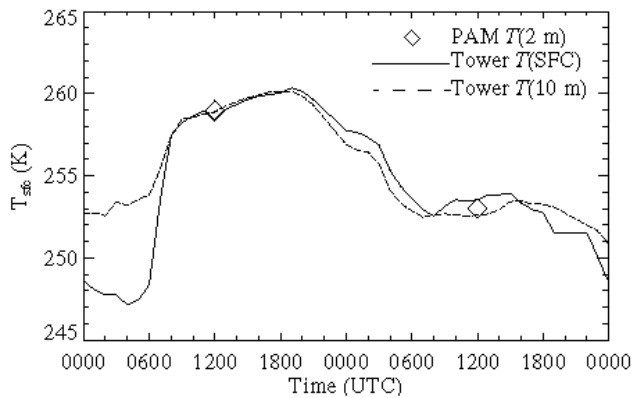
Figure 1. Surface temperature (solid), and air temperature at 10 m (dashed) from 10-m tower and air temperature at 2 m (diamonds) from flux-PAM station for a 2-day period beginning 14 November 1997.

employed to determine whether ice-phase or liquid-phase microphysical processes should be employed. This does not allow for the simulation of mixed-phase clouds.

The longwave radiative transfer is handled with the two-stream code used in Version 2 of the National Center for Atmospheric Research (NCAR) Community Climate Model (CCM2) (Briegleb 1992). The clouds are treated with bulk absorption coefficients that are a function of phase. The absorption coefficients for liquid and ice are 0.01 m^2 g^{-1} and 0.0735 m^2 g^{-1}, respectively.

The surface skin temperature of snow is specified from the observations obtained at the tower. An example of this is seen in Figure 1. The ocean surface temperature in leads is assumed to be -1.8° C. The ARCSyM column model is run for 23 days beginning 1 November 1997 to simulate the atmospheric and surface conditions observed at SHEBA. The model uses a sigma coordinate system (31 levels + the surface) with the highest resolution (a grid spacing of about 30 m just above the surface) in the lowest 1.5 km.

The large-scale advective tendencies of temperature, moisture and winds are obtained from European Centre for Medium Range Weather forecasting (ECMWF) data. The tendencies for each prognostic variable are 10 subdivided into a total tendency, T, and a physics tendency, P. The adiabatic or large-scale advective tendency (i.e., horizontal + vertical advection), A, which is needed by the column model, is simply obtained by A = T – P. Profiles of ECMWF tendencies averaged over the 23-day period of the simulation are shown in Figure 3. From the adiabatic tendency it is seen that advection tends to warm and moisten the profile, the exception being the drying occurring between 1 km to 2 km. The total tendencies are fairly small,
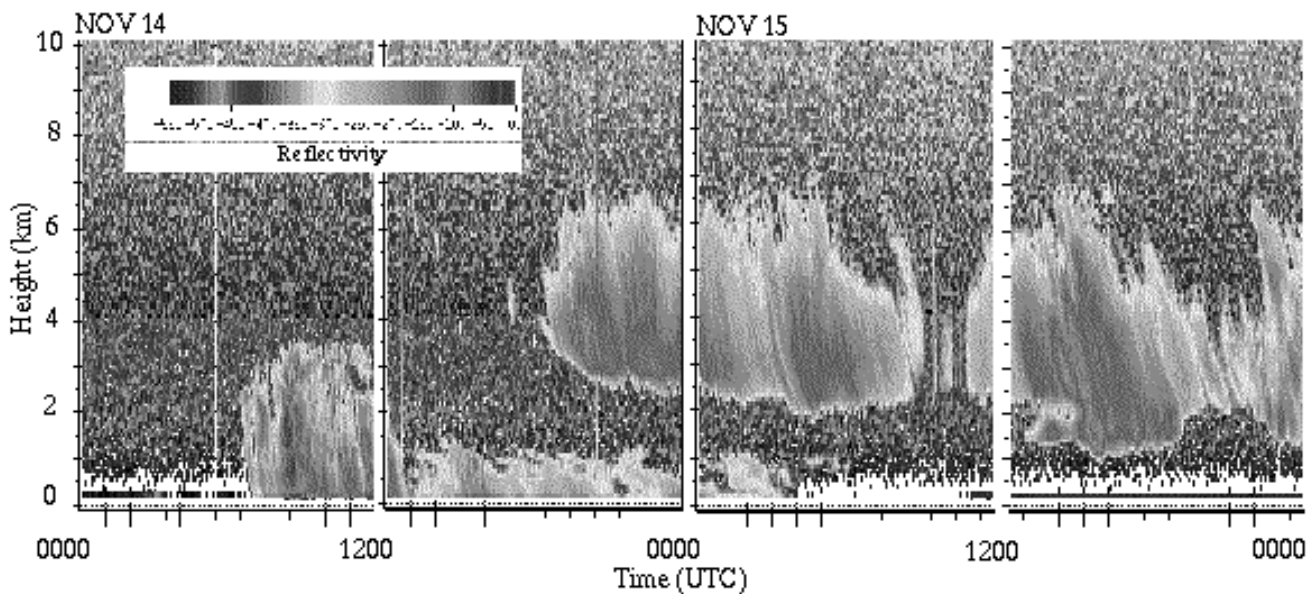
Figure 2. Reflectivity from 35-GHz cloud radar at SHEBA. Radar shows five distinct periods: 0000 UTC to 0600 UTC is clear, 0600 UTC to 1200 UTC precipitating cloud with tops of 3.5 km, 1200 UTC to 1900 UTC low precipitating cloud with top near 1 km, 1900 UTC to 0600 UTC dissipating low cloud below high cloud, and 0600 UTC to 0000 UTC high cloud only with some breaks. Lidar indicates that cloud between the surface and 1 km is mostly liquid and cloud above 2 km is mostly ice.
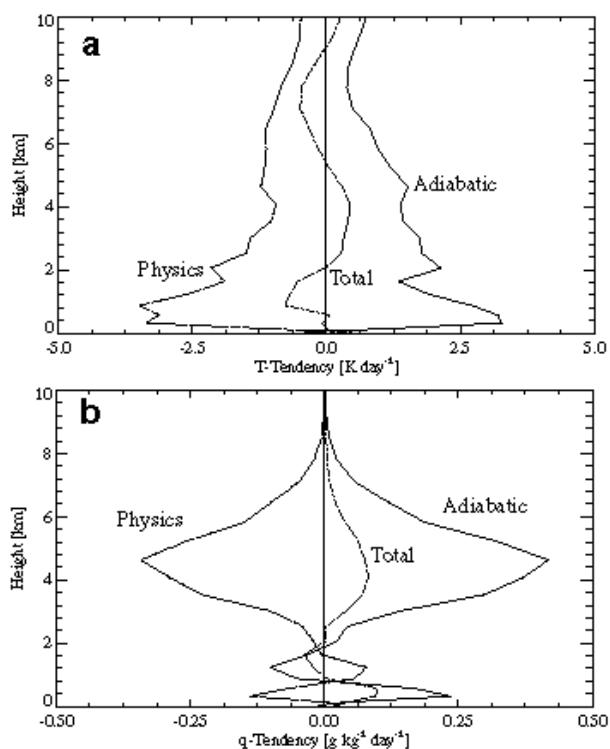
Figure 3. Profiles of (a) temperature tendencies and (b) water vapor mixing ratio tendencies obtained from ECMWF data. Three tendencies are shown: adiabatic (solid line), physics (dashed line), and total (dot-dashed line). Profiles are averages for the 1-23 November 1997 period. The adiabatic tendencies are used to force the model.

indicating that the warm moist advection into the SHEBA region is balanced by radiative cooling and cloud and precipitation formation.

Model Results

The SCM is run in two modes. The first mode is the sensitivity analysis, which includes several simulations with varying treatments of clouds and radiation. In the second mode, improvements determined from the sensitivity analysis are incorporated into the model, which is then run in a coupled mode using a thermodynamic sea ice model.

Sensitivity Analysis

Several sensitivity runs were performed to test radiative and microphysical parameterizations in the model. The temperature of phase transition, T_p, was varied between 250.16° K and 273.16° K, while the cloud absorption

coefficient was held constant at the value for ice. Results for T_p of 255.16° K and 273.16° K are compared. Two longwave radiative transfer schemes are tested in ARCSyM, CCM2 and RRTM. The sensitivity of the simulations to the treatment of cloud radiative properties was tested using RRTM. Here, simulations using the bulk absorption coefficients of CCM2 and spectral absorption coefficients (Hu and Stamnes 1993; Key 1996) are compared. Each simulation is summarized in Table 1.

Table 1. Sensitivity studies.			
	RT Scheme	**T-Phase Transition**	**Cloud Absorption**
Baseline	CCM2	273.16	Bulk
M255	CCM2	255.16	Bulk
RTMC2C	RRTM	273.16	Bulk
RTMDC	RRTM	273.16	Spectral

The temperature of cloud phase transition, T_p, is an important parameter in these simulations. In the baseline run, the cloud field was composed entirely of ice while in the M255 run much of the low clouds (i.e., < 2 km) were liquid. This has a significant impact on the vertical structure and total amount of condensed water in the atmospheric column (Figure 4). The amount of cloud water present in the low cloud layer has increased substantially in the M255 run. The low cloud layer also persists 6 hours longer in the M255 run. In addition, the amount of cloud water in the upper cloud layer is noticeably reduced while the vertical extent of the precipitation has increased. The low cloud in the M255 run is composed entirely of liquid while the high cloud is still just ice.

The changes in cloud water amount and cloud lifetime affect the downwelling longwave radiation (DLWR) at the surface (Figure 5). The DLWR is over 80 W m^{-2} greater in the M255 run than in the baseline run during the period from 0300-1800 UTC. The DLWR would have increased further had the bulk absorption coefficient for liquid been used. The DLWR in the M255 run becomes less than in the baseline case after 1900 UTC (by as much as 40 W m^{-2}) due to the reduced cloud water in the high cloud layer. The trends in the M255 run match the observations better than those in the baseline case, implying that 255° K is a more realistic temperature of phase transition.

The difference in the two simulations using different radiative transfer schemes is seen by comparing the baseline and RTMC2C runs (Figure 5). It is seen that the DLWR is greater when the RRTM scheme is used. This was true throughout the simulation with the CCM2 being on average about 20 W m^{-2} less than RRTM. The "bias" was greatest under clear skies or when low clouds were present
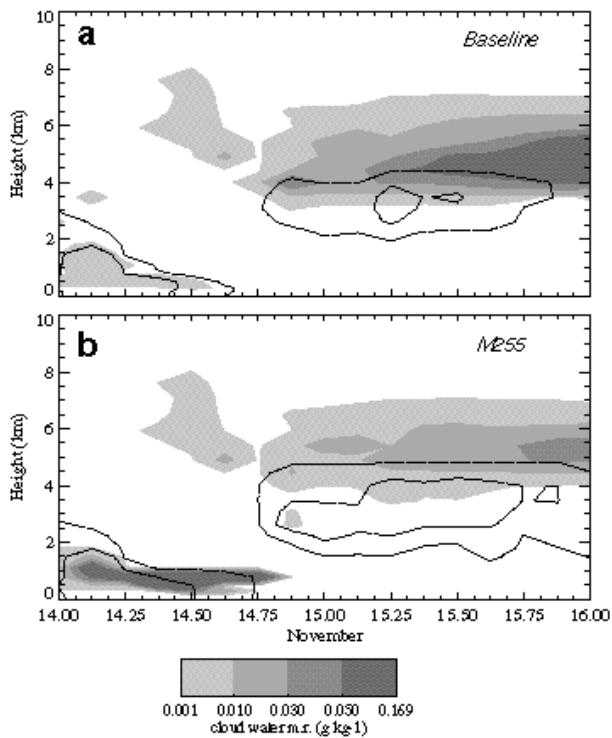
Figure 4. Time-height plots of cloud water mixing ratio (gray scale) and precipitation water mixing ratio (dashed contours) for (a) baseline and (b) M255 simulations. Darkest shading indicates regions where cloud water mixing ratio exceeds 0.05 g kg^{-1}.

and somewhat reduced when high clouds were present (Figure 5). This bias has been related to differences in the treatment of clear-sky gaseous absorption in the two radiative transfer schemes.

Comparing the two treatments of cloud absorption coefficient in RRTM also reveals a consistent offset. The use of spectrally dependent absorption coefficients results in a reduction in the DLWR compared with the bulk treatment. The time series of DLWR in the spectral treatment is similar to that obtained in the baseline case, which used CCM2 and bulk cloud absorption. Since the clouds were assumed to be all ice in these runs, it may be inferred that the bulk absorption coefficient for ice in CCM2 is too large.

Coupled Atmosphere/Sea Ice Simulation

Using results from the sensitivity studies, a determination of the best possible combination of parameterizations is made for use in a run with a coupled sea ice surface. For this simulation the temperature of phase transition is set to 255.16° K, the RRTM scheme is used with a spectral
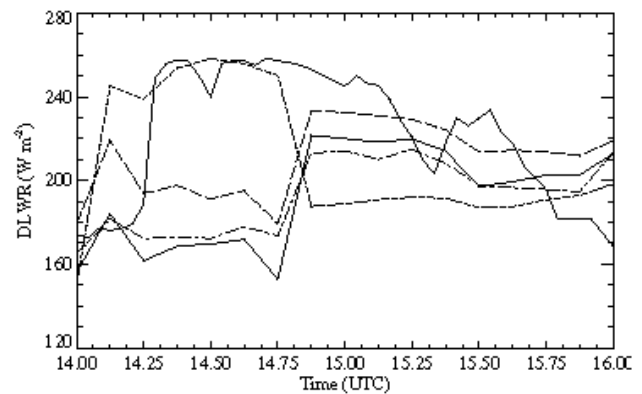

Figure 5. Downward longwave radiative flux at the surface for the Baseline case (solid line), M255 (short dashed line), RTMC2C (long dashed line), RTMDC (dot-dashed line) and Observed (thick solid line).

treatment of cloud absorption coefficients. The surface temperature is obtained using the thermodynamic sea ice model of Parkinson and Washington (1979).

The simulated cloud and precipitation water fields are shown in Figure 6. The liquid water layers stand out as having the larger cloud water mixing ratio maxima. Liquid water is present throughout the lowest 2 km of the atmosphere and is found as high as 4 km during a warm period between 10 and 13 November. High ice clouds (between 5 km and 8 km) occur more often than low liquid clouds (between 0 km and 2 km). The upper cloud layers have ice water mixing ratios of less than 0.05 g kg^{-1} while the lower cloud layers have liquid water mixing ratios of up to 0.16 g kg^{-1}. There are four precipitation events that reach the surface. This compares well with the observations while the intensity of the events is underestimated (see Pinto et al. 1998).

The net longwave radiative flux at the surface is an important component of the surface energy budget (SEB). The modeled net longwave radiation (LWR) at the surface varies between -65 W m^{-2} and +10 W m^{-2} with an average value of -35 W m^{-2}. The observed net LWR has a similar range but many more excursions above 0 W m^{-2} with a mean value of -21 W m^{-2}. The reason for this discrepancy is related to underpredictions in the cloud water amount and the occurrence of cloud, or errors in the assumed cloud phase for radiation calculations. An example of underpredicted cloud water amount is marked on the plots in Figure 6. It is seen that cloud is present in the model and the modeled net LWR flux is increased over clear-sky values (see 17 to 19 November) but not as much as observed. This occurs repeatedly toward the end of the simulation as well.
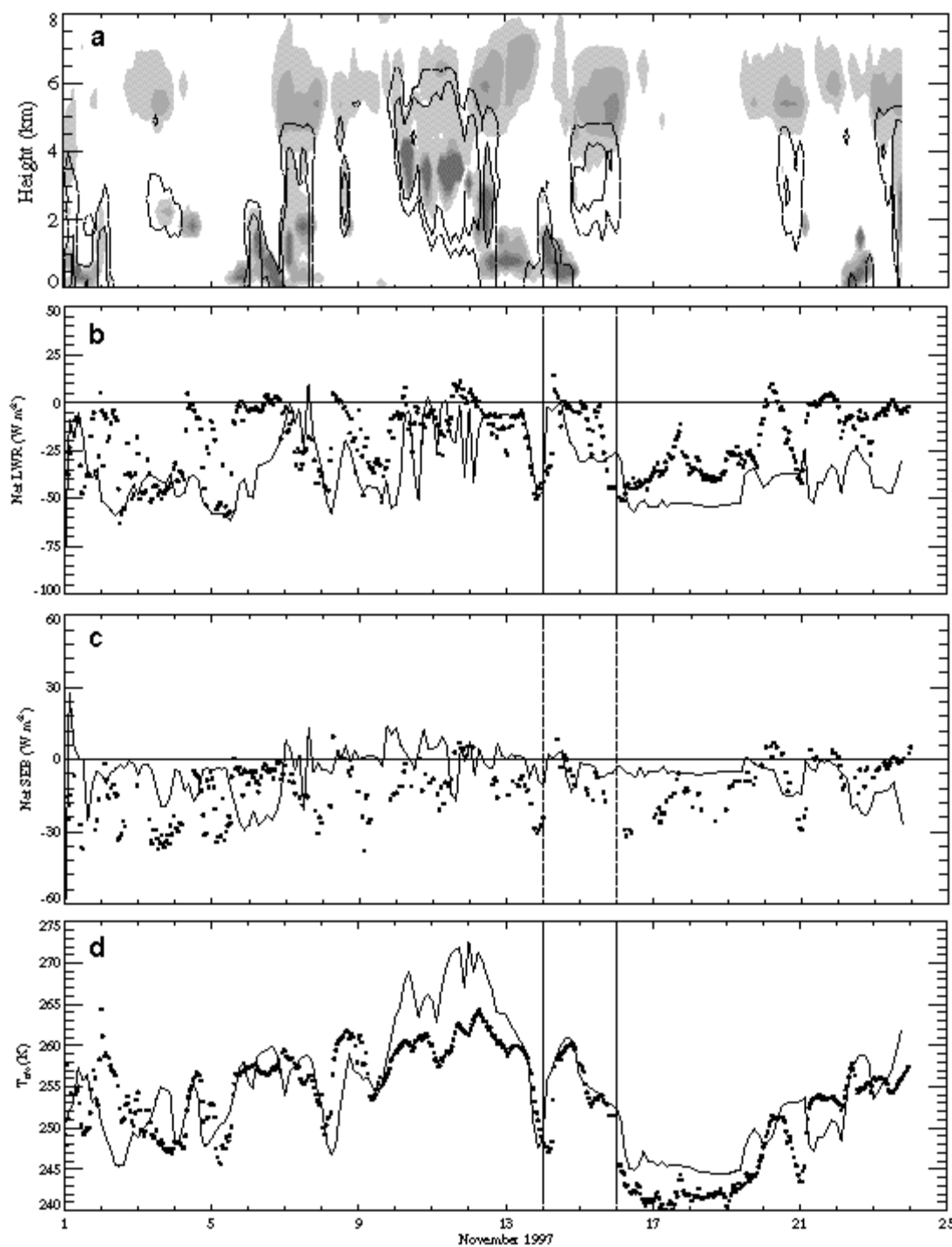
Figure 6. Time series of (a) cloud water mixing ratio (gray scale, 0,001, 0.01, 0.03, 0.05, > 0.05 g kg-1) and precipitation mixing ratio (dashed contours – 0.001 g kg-1 and solid contours – 0.01 g kg-1) as a function of height. Time series of (b) net longwave radiation, (c) net SEB (Net LWR + Sensible + Latent + Conductive Flux) and (d) surface temperature obtained from the coupled simulation (solid line) and observed at the 10-m tower (dots). The vertical lines denote the period of time discussed in the sensitivity analysis section.

Errors in the net LWR often have a large impact on the net SEB. After initial spin up, the modeled net SEB varies between -30 W m^{-2} and +10 W m^{-2} with a mean of -5.8 W m^{-2}. The observed net SEB is often significantly less than modeled with a range of -40 W m^{-2} to + 10 W m^{-2} and a mean of -12.9 W m^{-2}. This general positive bias in the model has several exceptions, particularly during two periods (6 November and 20 to 24 November) when either the modeled vertical distribution of cloud water is wrong or the modeled clouds are not optically thick enough (likely due to wrongly assuming ice-phase microphysics and ice-phase cloud radiative properties).

The modeled T_{sfc}, shown in Figure 6d indicates that the general trends are reproduced fairly well while individual events may not be. The largest error occurred during a 3-day period beginning 10 November when the modeled T_{sfc} are much too high (i.e., 3° K to 8° K too warm). The modeled and observed T_{sfc} traces are fairly well correlated for the most part (an exception is readily seen at 2 November). The mean modeled T_{sfc} is 1.4° K warmer than the average T_{sfc}.

Summary and Conclusions

Simulations of the November 1997 period of SHEBA were very sensitive to the treatment of clouds. This was particularly evident in the longwave radiation at the surface. The results were very sensitive to the temperature of phase transition, T_p, of clouds. It was found that a more realistic simulation was obtained when the temperature at which ice clouds were allowed to form was lowered to 255.16° K. This lower T_p allowed for the occurrence of supercooled liquid water clouds. Supercooled liquid and mixed-phase clouds are known to occur with some regularity below 4 km in the Arctic in autumn (e.g., Pinto and Curry 1998). The modeled liquid water clouds in the coupled run were optically thicker due to an increased amount of condensate present and using the spectral absorption coefficient for liquid instead of ice. The modeled net longwave flux at the surface was 14 W m^{-2} (67%) less than observed in the coupled simulation; however, errors in the modeled surface temperature contribute about 6 W m^{-2} to the total error. It is clear that a more physically based treatment of cloud-phase changes, allowing for the occurrence of mixed-phase clouds needs be developed from observations and model process studies to improve Arctic winter simulations. In addition, the radiative properties of Arctic clouds need to be better understood. Data from the combined SHEBA and FIRE.ACE field experiments should help address these issues.

Acknowledgments

References

Briegleb, B. P., 1992: Longwave band model for thermal radiation in climate studies. *J. Geophys. Res.*, **97**, 11,475-11,485.

Hsie, E. Y., R. A. Anthes, and D. Keeyser, 1984: Numerical simulation of frontogenesis in a moist atmosphere. *J. Atmos. Sci.*, **41**, 2581-2594.

Hu, X. Y., and K. Stamnes, 1993: An accurate parameterization of the radiative properties of water clouds suitable for use in climate models. *J. Climate*, **6**, 728-742.

Key, J., 1996: Streamer User's Guide, Technical Report 96-01, Dept. of Geography, Boston University, 75 pp.

Lynch, A. H., W. L. Chapman, J. E. Walsh, and G. Weller, 1995: Development of a regional climate model of the western Arctic. *J. Climate*, **8**, 1555-1570.

Mlawer, E. J., S. J. Taubman, P. D. Brown, M. J. Iacono, and S. A. Clough, 1997: Radiative transfer for inhomogeneous atmospheres: RRTM, a validated correlated-k model for the longwave. *J. Geophys. Res.*, **102**, 16,663-16,682.

Parkinson and Washington, 1979: A large-scale numerical model of sea ice. *J. Geophys. Res.*, **84**, 311-337.

Pinto, J. O., 1998: Autumnal mixed-phase cloudy boundary layers in the Arctic. *J. Atmos. Sci.*, **55**, 2016-2038.

Pinto, J. O., J. A. Curry, A. H. Lynch, and O. Persson, 1998: Modeling clouds and radiation for the November 1997 period of SHEBA using a column climate model. *J. Geophys. Res.*, accepted.

Other Publications in Progress

Pinto, J. O., and J. A. Curry, 1998: Microphysical and radiative properties of clouds over the Beaufort Sea in autumn. In preparation.